applied sciences

MDPI

Article

Study of the Deformation by Compression of a Premolar with and Without Ceramic Restoration Using Speckle Optical Interferometry

Erik Baradit [1,*], Jorge Gutiérrez [2], Miguel Yáñez [3], Claudio Sumonte [2] and Cristhian Aguilera [4]

[1] Physics Department, University of Bío-Bío, Av. Collao 1202, Concepción 4051381, Chile
[2] Department of Odontology, Universidad del Desarrollo, Ainavillo 456, Concepción 4070001, Chile; jgutierrez@ingenieros.udd.cl (J.G.); c.sumonte@udd.cl (C.S.)
[3] Department of Statistics, University of Bío-Bío, Av. Collao 1202, Concepción 4051381, Chile; myanez@ubiobio.cl
[4] Department of Electrical and Electronic Engineering, University of Bío-Bío, Av. Collao 1202, Concepción 4051381, Chile; cristhia@ubiobio.cl
* Correspondence: ebaradit@ubiobio.cl; Tel.: +56-41-3111306

Abstract

This work aimed to quantify axial deformations of a human premolar during occlusion with its antagonist and to compare them with the same premolar restored with a ceramic crown. The deformations were put under stress using a mechanical press with a force ranging from 1 to 100 Newtons. These deformations were quantified using the optical interferometry technique with a laser source (633 nm, 0.95 mW). Using a CMOS camera, interference fringes were obtained, stored, and subsequently processed. The premolars were restored with Cerasmart GC ceramic, using the CAD-CAM system. The average deformations of healthy premolars were found to be in a range of 0.69 to 1.74 μm, while the restored ones were deformed in a range of 0.53 to 1.10 μm. The results of this work showed that the Cerasmart ceramic material had similar properties to those of the natural tooth for small forces. However, for higher forces, the ceramics increased the coronal stiffness of the tooth. This modified the optimal combination of stiffness, strength, and resilience between the enamel and dentin, causing a decrease in the tooth's ability to dissipate energy; therefore, the tooth could receive more stress. The observed mechanical properties lead to the conclusion that the Cerasmart material can be indicated for the restoration of anterior and premolar teeth in most cases where a fixed prosthesis is required.

Keywords: axial deformation; dentistry; ceramic composite; optics interferometry

Academic Editor: Vittorio Checchi

Received: 2 August 2025
Revised: 19 September 2025
Accepted: 20 September 2025
Published: 4 October 2025

Citation: Baradit, E.; Gutiérrez, J.; Yáñez, M.; Sumonte, C.; Aguilera, C. Study of the Deformation by Compression of a Premolar with and Without Ceramic Restoration Using Speckle Optical Interferometry. *Appl. Sci.* **2025**, *15*, 10708. https://doi.org/10.3390/app151910708

1. Introduction

Over the last 20 years, the efforts of researchers and developers of new dental materials have focused on reproducing the original biomechanics of lost teeth [1]. Due to the limited knowledge available, in modern dentistry, it is increasingly important to obtain evidence of natural tooth deformations during occlusion with the antagonist, since the main objective is to offer highly personalized restorative treatments. This study aims to investigate the deformations of a healthy premolar and then compare these with those experienced by a Cerasmart GC ceramic crown, manufactured with CAD-CAM technology. An experiment was designed to study the deformations in a similar way to what happens in the mouth, where the normal condition of a premolar's occlusion with its antagonist is emulated, measuring these deformations using the speckle optical interferometry technique. The

challenge was to observe the axial deformation of premolars in an occlusion process that was as close to reality as possible. This made it possible to compare the deformations experienced by a ceramic crown with those of a healthy premolar.

Lately, most of the studies aimed at quantifying the mechanical properties of human teeth have been those based on non-destructive techniques, since, unlike traditional material tests, which require the material's breaking point, they allow characterizing teeth without having to destroy them.

Among these, one of the most widely used to study occlusion is optical coherence tomography [2]. With this, it has been observed that maxillary teeth have a more facial position and the areas of their central fossa occlude on the cusps of the mandibular teeth. Similarly, the maxillary lingual cusps are in occlusion with the central fossa areas of the mandibular teeth [3]. It has also been determined that the normal human masticatory process varies depending on the individual's age, sex, and, even more so, if the patient suffers from a given occlusal pathology. This technique has allowed reaching the conclusion that the bonding strength between dentin and a composite resin decreases over time [4].

Using finite element analysis [5], it has been shown that during occlusion, a healthy premolar will present deflection in its crown, producing traction forces on the palatal half of the tooth, and compression forces on the vestibular half [6]. These studies conclude that an optimal combination of the rigidity and strength of the enamel with the resilience of the dentin will allow the natural tooth to adequately withstand masticatory processes. Other non-destructive methods have used optical interferometry as a powerful technique to quantify deformations and stresses in both teeth and restorative materials.

Among these methods is Digital Moiré Interferometry (DMI), where it has been observed that, during the compression of a human tooth, the enamel shows marked deformation gradients in the lateral direction, and the coronal dentin shows marked axial gradients [7]. In the same line of optical interferometry is the Electronic Speckle Pattern Interferometry (ESPI). This technique has been used to study, for example, the polymerization contraction of composite resins, where it has been possible to quantify the deformation of the material compared to the tooth walls [8,9]. The deformations of human teeth surfaces have been quantified [10] using this same evaluation method, where it has been shown that the maximum deformations of premolars are recorded in the occlusal third, reaching values ranging from 0.3 [μm] to 5 [μm], while the axial deformations range from 0.3 [μm] to 2.7 [μm], in the middle third of the tooth [11]. ESPI has also been used to quantify deformations suffered by a tooth restored with a ceramic crown [12], proving that when removing the enamel from a premolar and then replacing it with a ceramic crown, the tooth and the material deform differently. Other studies, based on the use of extensometer gauges [13,14], have proven that enamel is the tissue that contributes the most to tooth strength. These and other investigations have tried to emulate the oral conditions of the teeth, and have provided relevant information for both material developers and dentists, who together seek to expand the limits of restorative work, allowing, on one hand, new material formulations, and, on the other, perfecting the rehabilitation techniques applied by the dentist.

The speckle optical interferometry technique is widely used to obtain information about displacements, deformations, or vibrations experienced by an object when under the action of a mechanical or thermal load. This technique uses an optical interferometer where the object under study is located on one of its arms. The light beam from a coherent source is reflected off the object and overlaps with a reference beam, resulting in an interference pattern known as a speckle pattern. This setup allowed us to compare the deformations experienced by a ceramic crown with those of a healthy premolar. The application of an external load to the object causes a change in the speckle pattern, and its overlapping

produces interference fringes whose number and arrangement contain information about the deformation experienced by the object. In this study, a setup was used that allowed the occlusion process to be emulated as realistically as possible. Thus, the premolars were tested directly with their antagonists using a non-destructive method, unlike other studies in which the premolars are tested under pressure from a press. It was found that Cerasmart exhibits deformations similar to those of natural teeth for forces below 83.45 N. As is known, the intensity from the overlapping of two beams is

$$I = I_1 + I_2 + 2\sqrt{I_1 I_2}\, cos\, \delta \quad (1)$$

where δ is the phase difference between the beams and I_1 and I_2 are the corresponding intensities [15]. Depending on this phase difference, the resulting light intensity can lead to constructive and destructive interference. Generally, this phase difference is written as

$$\delta = \left(\vec{k_2} - \vec{k_1}\right)\vec{d} \quad (2)$$

where $\vec{k_1}$ and $\vec{k_2}$ are the propagation vectors [15] and $\vec{d}$ is the displacement vector in three dimensions [16]. For the case of axial deformation, the phase difference δ, introduced by the deformation, is given by

$$\delta = \left(\vec{k_2} - \vec{k_1}\right)\vec{d} = \frac{2\pi}{\lambda} 2d_z \quad (3)$$

where d_z is the axial displacement and λ is the wavelength. Considering that the total constructive interference appears when $\delta = 2\pi n$, where n is an integer, hence

$$\frac{2\pi}{\lambda} 2d_z = 2\pi n \quad (4)$$

and, therefore, the displacements on the axial axis are quantified by the following formula:

$$d_z = \frac{n\lambda}{2} \quad (5)$$

2. Materials and Methods

2.1. Preparation of Healthy Premolars

Ten lower and five upper caries-free premolars extracted by orthodontic prescription were used. The teeth were placed in chloramine, and then the soft root tissue was cleaned and removed, taking care not to alter the structure of the dental crown. The clean dental samples were stored in a high-density polyethylene container with a hermetic seal, in chloramine, and kept in a refrigerator at 4 °C. They were then mounted on a mechanical testing machine specially designed to replicate the normal occlusion of the lower premolars with their antagonist, following the tripoidism criterion.

2.2. Preparation of the CAD-CAM Ceramic Crown

Once the healthy premolars were tested, all the samples were taken to the laboratory for the design of the restoration and the manufacture of the crown with Cerasmart block, manufactured by the company, GC Germany (Bad Homburg, Germany). The digitization work began with the 3D scanning of the premolars to obtain the anatomical reference that the ceramic restoration must comply with. An Amann Girrbach MAP400 3D scanner (Amann Girrbach AG, Maeder, Austria) was used for this purpose. A digitized premolar is shown in Figure 1.

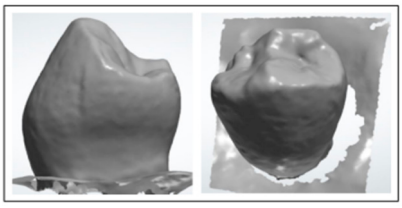

Figure 1. Anatomy scan of a premolar.

After being scanned, the samples were arranged for the carving of the preparations or stumps that would receive the restorations, machined with the Cerasmart block. For this stage, silicone impressions were taken before carving, to have a negative of the tooth and thus measure the wear thickness, as shown in Figure 2, thus ensuring that all the samples are as similar as possible.

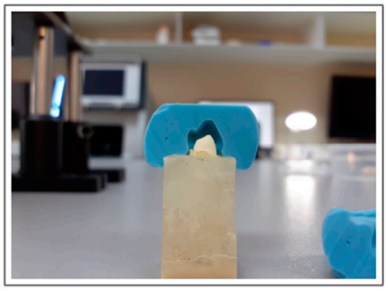

Figure 2. Silicone impression obtained from the anatomy of the premolar before carving.

High-speed diamond cutters cooled by air and water were used for the carving, so as not to fracture the teeth. The stumps for 3 premolars are shown in Figure 3.

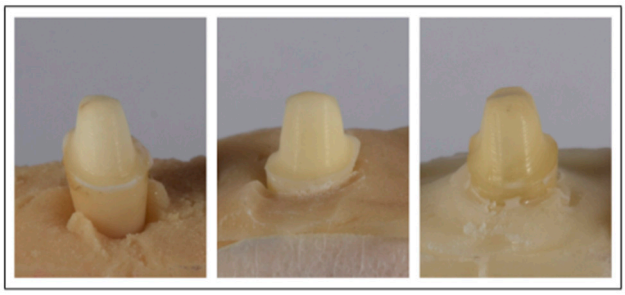

Figure 3. Carving of healthy premolar stumps.

Once the stumps were finished in each of the samples, they were scanned again and digitized in the laboratory to proceed with the design of each of the restorations (Figure 4a).

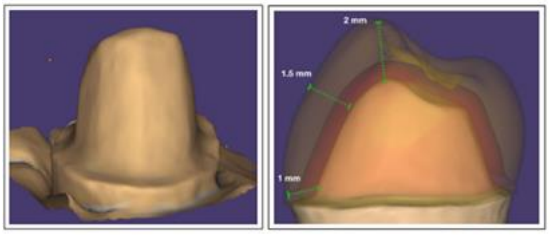

(**a**) (**b**)

Figure 4. (**a**). Digitization of the carved stump. (**b**). Ceramic crown thicknesses.

The design of the restorations was carried out using Exocad dentalcad 2.4 Provdiv software, taking care of the appropriate material thicknesses and considering the wear

previously made for the stump. A scanned image with the thicknesses of the ceramic crowns is shown in Figure 4b. The design of each structure was sent to the digital laboratory to be machined with the Roland DWX51 4-axis milling machine (Roland DGA, Irvine, CA, USA). The freshly milled crowns are shown in Figure 5.

Figure 5. Ceramic crowns after milling.

After being machined, the restorations were cemented to each of the prepared samples, using a universal, self-adhesive, and self-polymerizable resin cement (Relyx U200 3M Center, 2510 Conway Avenue, St. Paul, MN 55144, USA), whose simplified protocol avoids applying acids and extra bonding to dental preparations [17,18]. Before the cement was applied, the restored surface was treated to give micro-roughness to the material and thus obtain greater adhesion. A portable BioArt brand micro-sandblaster (BioArt Laboratories, Eindhoven, The Netherlands) was used for this. It applied an abrasive air jet with 30 µm aluminum oxide particles for 15 s at 2 bar pressure and a distance of 10 mm. Then, the samples were cleaned with 20% orthophosphoric acid for 20 s, and washed and dried with oil-free air for 5 s. After performing the surface protocol, the cementing material was injected, and the excess was removed with a microbrush. To foster the cement's polymerization, a 3M Espe Elipar 2500 brand photocuring lamp (3M Elipar DeepCure-S LED Curing Light, 3M Oral Care 2510 Conway Avenue, St. Paul, MN 55144-1000, USA) was used, applying light for 4 s on each side of the restoration.

2.3. Mechanical Device

A mechanical press was manufactured consisting of two gears with 40 and 80 mm diameters, supported by two columns welded perpendicularly to a metal base, and a rotating screw attached to the larger diameter gear. The forces applied were controlled by an electric motor, programmed in Assembly language. These forces were quantified by means of a load cell, whose readings were processed by an Arduino-based system. To emulate human masticatory conditions, an upper premolar was attached to the tip of the screw and occluded respecting the normal bite patterns to comply with at least two contact points sought in the therapeutic occlusal tripoidism (Figure 6a,b).

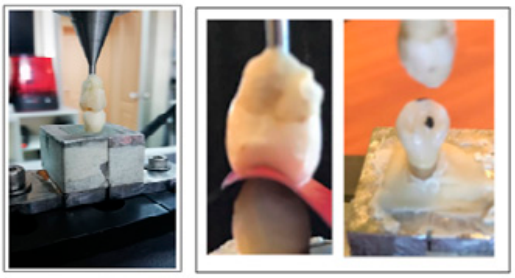

(**a**) (**b**)

Figure 6. (**a**). Occlusion of premolars. (**b**). Occlusion of premolars.

The objective was to ensure that the pieces being tested had uniform contact in at least those two points with the antagonist and thus stabilize the bite. These contact points were verified in all the samples, both on the teeth and on the restorations, using 8-micron-thick articular paper for this (Figure 6b). To control the loads on the teeth, consecutive rotational tightening of the press gear was performed using the compression loads indicated in Table 1.

Table 1. Mean and standard deviations of the deformations of the premolars and the ceramic crown.

Forces Applied [N]	Premolar Deformation [µm]		Ceramic Block Deformation [µm]	
	Mean	SD	Mean	SD
80.16	0.69630	0.13345	0.53805	0.21362
83.45	0.79125	0.22379	0.63300	0.14919
86.73	1.04445	0.26056	0.85455	0.15288
89.77	1.20270	0.29084	0.88620	0.20017
91.83	1.36095	0.26056	1.07610	0.21362
94.28	1.61415	0.27712	1.07610	0.16344
95.75	1.74075	0.22379	1.10775	0.22379

2.4. Experimental Optical Arrangement

The experimental arrangement used in this work is a Twyman and Green interferometer, which is a modified Michelson interferometer [19], where one of its mirrors was replaced by the dental specimen being tested (Figure 7a). The interferometer, Figure 7b, consists of a Helium–Neon (He-Ne) laser, with a wavelength of $\lambda = 633$ nm and 0.95 mW in power. The optics used to condition the beam include a spatial filter, comprising a convergent lens and an aperture to obtain a beam with a Gaussian distribution. It also has a 200 mm focus divergent lens to expand the beam, a beam splitter, and a mirror to reflect the beam to the beam splitter and then to the sample. The setup was carried out in an optics laboratory isolated from the external environment at controlled room temperature and on a Thorlabs anti-vibration optical table. Previously, the mechanical assembly was anchored to the optical table, adjusting the position of the tooth and the laser light source. The position of the premolar was defined by the occlusal tripoidism of the antagonist tooth. To acquire the speckle images, a Basler brand camera (Basler, Ahrensburg, Germany) with a CMOS technology sensor and a resolution of 2590 × 1942 pixels was used.

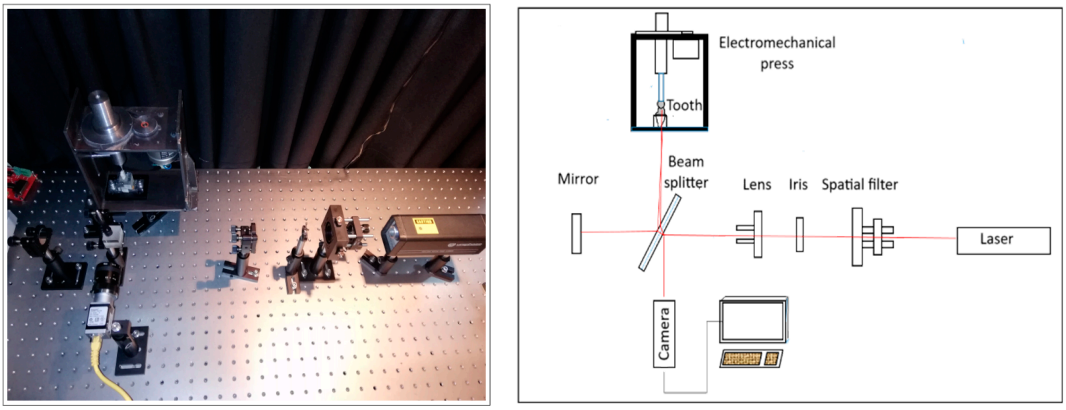

(**a**) (**b**)

Figure 7. (**a**). Interferometer for measuring axial deformation. (**b**). Schematic of the experimental setup.

2.5. Measurements

To experiment with the premolars, the teeth were compressed until the calibration zero point was reached, a starting preload that turned out to be 77.8 N. The teeth were

then compressed by increasing the press load following the values indicated in Table 1. New speckle images were obtained for each of the loads mentioned. These images were subsequently processed using a Python 3.8 program, where the first image was replaced with the following ones, obtaining interference fringes, whereby the axial deformations experienced during the occlusion process were estimated.

3. Results and Discussion

Interference fringes are shown in Figure 8 for both a healthy and a restored tooth, obtained as a result of image processing for different compression forces.

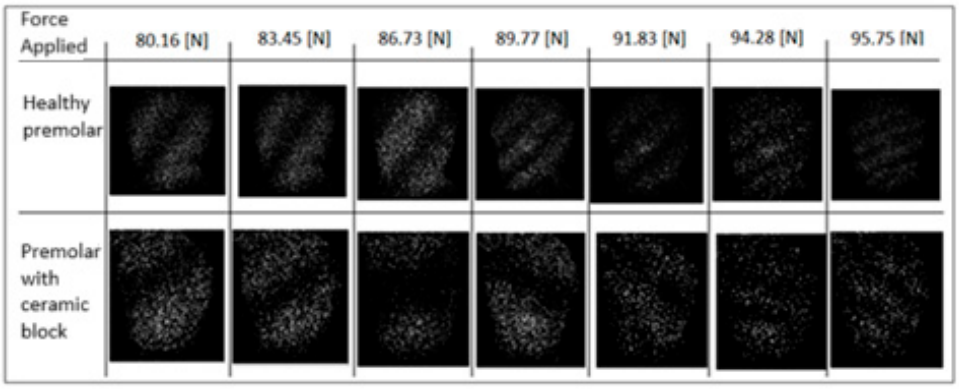

Figure 8. Interference fringes of the healthy premolar and subsequently restored with a ceramic crown.

A change in the inclination of the interference fringes can be observed in Figure 8, which is a rotation of the tooth as the occlusion load increases. As can be seen, this rotation occurs to a greater extent for the piece restored with ceramics. This rotation is shown in Figures 9 and 10 through the change in the direction of the yellow arrows perpendicular to the fringes. The red arrow indicates the initial orientation.

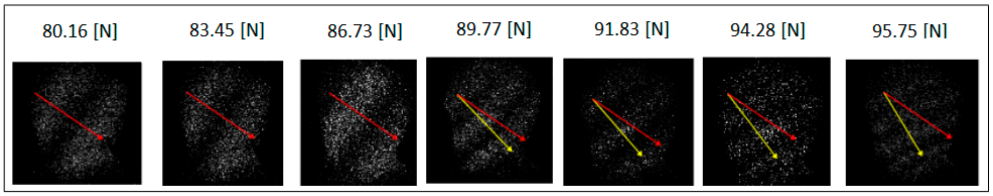

Figure 9. Propagation of forces on the vestibular surface of the healthy premolar.

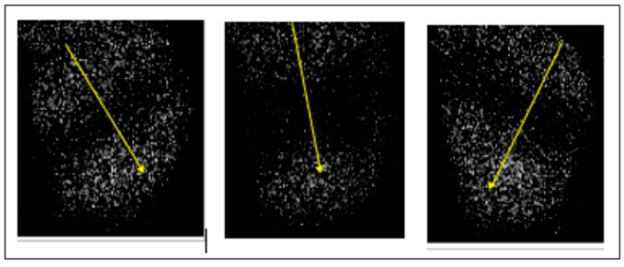

Figure 10. Propagation of the forces on the vestibular surface of the premolar restored with the ceramic crown for three consecutive presses.

The results obtained through Equation (5) for the averages of the teeth's axial deformations with and without ceramic restoration under different loads are shown in Table 1. As can be seen from this table, the teeth with ceramic restoration rotate more under compression forces but suffer less axial deformation than healthy teeth due to their greater rigidity. The average values of these deformations are shown in Figure 11.

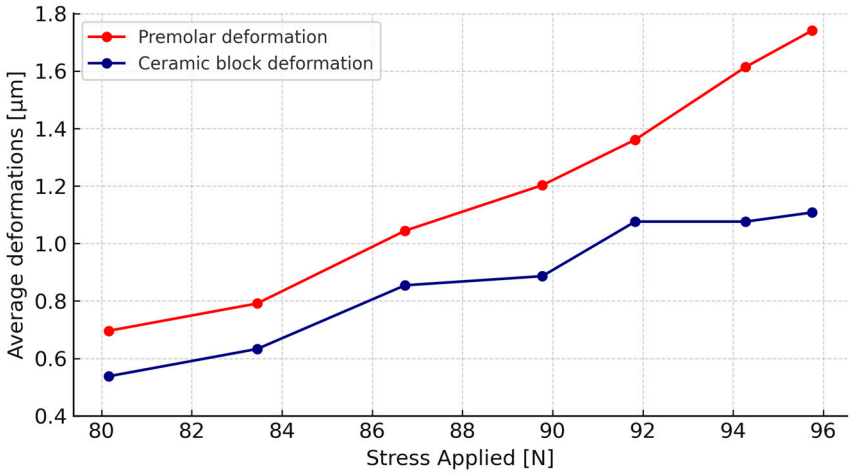

Figure 11. Average axial deformations of the vestibular surface of the premolars and ceramic crowns for different tightening.

To check if there are statistically significant differences between these average deformations, the non-parametric Wilcoxon test was applied for related samples [20], finding that for forces of 80.16 N and 83.45 N, the average deformations do not differ between healthy premolars and premolars with a ceramic crown. For forces of 86.73 and 89.77 N, the average deformations differ significantly between healthy premolars and premolars with a ceramic crown. Finally, for forces of 91.83 N, 94.28 N, and 95.75 N, there is a highly significant difference between the average deformations of healthy premolars and premolars with a ceramic crown. The results of this test are shown in Table 2.

Table 2. Wilcoxon test for related strain samples.

Forces Applied [N]	Statistic Z	Effect Size	*p*-Value	
80.16	−1.518	0.48	0.129	n.s.
83.45	−1.633	0.52	0.102	n.s.
86.73	−2.121	0.67	0.034	*
89.77	−2.308	0.73	0.021	*
91.83	−2.714	0.86	0.007	**
94.28	−2.859	0.90	0.004	**
95.75	−2.694	0.85	0.007	**

n.s. There are no statistically significant differences. * There is a statistically significant difference (p-value < 0.05), ** There are highly significant differences (p-value < 0.01).

The results of this work showed that, for restorations in anterior teeth, where occlusal forces are less intense, Cerasmart may be a suitable material given that it exhibits deformations similar to those of natural teeth. As the experimental results show, the correlation fringes on the enamel of healthy premolars are inclined and slightly curved. This behavior is due to the curved anatomy of the tooth's vestibular surface, as well as the points where the upper premolar occludes over the lower premolar under study. The change of direction of the fringes is due to the rotation of the crown relative to the tooth that supports it, which causes the point of concentration of greatest stress produced by the initial occlusion to change, as shown in Figure 10. These results are similar to those obtained by Barak et al. [11], who determined that the axial deformations of the vestibular surface of lower premolars are in the range of 0.3 to 2.7 µm, in the middle third of the tooth, and also the studies of Valin et al. [21], who determined that upper premolars subjected to compressive loads in a range of 25 to 100 N exhibited deformations between 1.4 to 1.85 µm. According to the results, it can be seen that by removing the natural enamel of the tooth and then restoring it with Cerasmart ceramics, its strength to axial deformation increases, i.e., the

ability of the tooth to dissipate energy and therefore concentrate more efforts decreases, coinciding with the observations of Fages et al. [12].

The main limitation in this work was the difficulty of obtaining a larger number of healthy premolars extracted on orthodontic prescription. On the other hand, the optical interferometry technique is widely used for studies of deformations in different types of materials, so no limitations are observed in this regard. There are no limitations in terms of materials, as manufacturers are willing to provide their products for evaluation. Future guidelines include studying lateral deformations of premolars from distal to mesial and from occlusal to cervical. It is also planned to extend these studies to posterior teeth and other materials.

4. Conclusions

In this study, Cerasmart was selected due to its ability to emulate dentin because of its similar modulus of elasticity, which promotes harmonious biomechanical interaction between the restoration and the remaining dental tissue. It should be noted that these results cannot be extrapolated to other widely used materials, such as lithium disilicate and zirconia, because their mechanical properties are different.

The axial deformations obtained from the central third of the healthy premolar's vestibular surface under compressive forces were between 0.69 and 1.74 microns, for between two and six interference fringes. The axial deformations of the restored premolar's ceramic crown under the same compressive forces were found to be between 0.53 and 1.1 microns, for one to four fringes. It was found that for compressive forces between 86.73 and 95.75 N, the average deformations of the restored premolars with a ceramic crown are significantly lower than those obtained with healthy premolars. On the other hand, the deformations obtained in premolars under occlusal forces with their antagonist showed a uniform stress distribution, confirming the homogeneity of the ceramic material. It is therefore concluded that the ceramic material increases the coronal rigidity of the natural tooth, which modifies the optimal combination of rigidity, strength, and resilience between enamel and dentin. This paper shows the potential of the optical interferometry technique in studying deformations in premolars with and without ceramic restoration. These results are preliminary laboratory-scale work, but at the same time, they show the potential of optical interferometry for this type of study. We hope that future guidelines will include studying lateral deformations of premolars from distal to mesial and from occlusal to cervical. It is also planned to extend these studies to posterior teeth, improve the setups, and use other materials.

Author Contributions: Conceptualization, E.B. and C.S.; methodology, J.G.; software, J.G.; formal analysis, C.A.; resources, J.G.; data curation, M.Y.; writing—original draft preparation, J.G.; writing—review and editing, E.B.; funding acquisition, E.B. All authors have read and agreed to the published version of the manuscript.

Funding: This research was carried out within the framework of the Grupo GI 152007/VC project and Regular project 132407, supported by the Research Department of the Universidad del Bío-Bío.

Institutional Review Board Statement: Not applicable.

Informed Consent Statement: Not applicable.

Data Availability Statement: The original contributions presented in this study are included in the article. Further inquiries can be directed to the corresponding author.

Acknowledgments: We would like to thank the Research Department of the Universidad del Bío Bío and the Faculty of Health Sciences of the Universidad del Desarrollo for their support. The authors also thank the ARVIDENT laboratory for their support in designing the crowns used in this work.

Conflicts of Interest: The authors declare no conflicts of interest.

Abbreviations

The following abbreviations are used in this manuscript:

DMI	Digital Moiré Interferometry
ESPI	Electronic Speckle Pattern Interferometry
CAD-CAM	Computer-Aided Design-Computer-Aided Manufacturing
µm	Micrometer
N	Newton
CMOS	Complementary Metal–Oxide–Semiconductor
GC	GC Corporation (Cerasmart material manufacturer)
He-Ne	Helium–Neon (laser type)

References

1. Magne, P.; Belser, U. *Restauraciones de Porcelana Adherida en Los Dientes Anteriores: Método Biomimético*; Editorial Quintessence: Barcelona, España, 2004; pp. 30–31.
2. Baumgartner, A.; Dichtl, S.; Hitzenberger, C.K.; Sattmann, H.; Robl, B.; Moritz, A.; Fercher, A.F.; Sperr, W. Polarization-sensitive optical coherence tomography of dental structures. *Caries Res.* **2000**, *34*, 59–69. [CrossRef] [PubMed]
3. Hwang, S.; Choi, Y.J.; Jung, S.; Kim, S.; Chung, C.J.; Kim, K.H. Posterior dental compensation and occlusal function in adults with different sagittal skeletal malocclusions. *Korean J. Orthod.* **2020**, *50*, 98–107. [CrossRef] [PubMed]
4. Marin, B.; Makishi, P.; Sadr, A.; Shimada, Y.; Sumi, Y.; Tagami, J.; Giannini, M. Evaluation of bulk-fill systems: Microtensile bond strength and non-destructive imaging of marginal adaptation. *Braz. Oral Res.* **2018**, *32*, e80.
5. Rivadeneira, C.; Bonifaz, E.A. Modelado de elementos finitos en dientes premolares. *ACI Av. En Cienc. E Ing.* **2013**, *5*. [CrossRef]
6. Robinson, D.; Aguilar, L.; Gatti, A.; Abduo, J.; Vee Sin Lee, P.; Ackland, D. Load response of the natural tooth and dental implant: A comparative biomechanics study. *J. Adv. Prosthodont.* **2019**, *11*, 169–178. [CrossRef] [PubMed]
7. Kishen, A.; Tan, K.; Asundi, A. Digital moiré interferometric investigations on the deformation gradients of enamel and dentine: An insight into non-carious cervical lesions. *J. Dent.* **2006**, *34*, 12–18. [CrossRef] [PubMed]
8. Campos, L.; Parra, D.; Vasconcelos, M.; Vaz, M.; Monteiro, J. DH and ESPI laser interferometry applied to the restoration shrinkage assessment. *Radiat. Phys. Chem.* **2014**, *94*, 190–193. [CrossRef]
9. Lang, H.; Rampado, M.; Müllejans, R.; Raab, W.H.M. Determination of the dynamics of restored teeth by 3D electronic speckle pattern interferometry. *Lasers Surg. Med.* **2004**, *34*, 300–309. [CrossRef] [PubMed]
10. Zaslansky, P.; Currey, J.; Friesem, A.; Weiner, S. Phase shifting speckle interferometry for determination of strain and Young's modulus of mineralized biological materials: A study of tooth dentin compression in water. *J. Biomed. Opt.* **2005**, *10*, 024020. [CrossRef] [PubMed]
11. Barak, M.; Geiger, S.; Chattah, N.; Shahar, R.; Weiner, S. Enamel Dictates Whole Tooth Deformation: A Finite Element Model Study Validated by a Metrology Method. Available online: https://www.sciencedirect.com/science/article/abs/pii/S1047847709002056 (accessed on 24 March 2025).
12. Fages, M.; Slangen, P.; Raynal, J.; Corn, S.; Turzo, K.; Margerit, J.; Cuisinier, F.J. Comparative mechanical behavior of dentin enamel and dentin ceramic junctions assessed by speckle interferometry (SI). *Dent. Mater.* **2012**, *28*, e229–e238. [CrossRef] [PubMed]
13. Mendes, J.; de Oliveira, A.; Souto, A.; Nishioka, R.; Bottino, M.; Rodrigues, V. Effect of Framework Type on the Biomechanical Behavior of Provisional Crowns: Strain Gauge and Finite Element Analyses. *Quintessence Int.* **2020**, *40*, e9–e18.
14. Araujo, F.; Favaro, L.; de Almeida, G.; Rodriguez, B.; Dantas, R.; Vinícius, P. Restorative material and loading type influence on the biomechanical behavior of wedge-shaped cervical lesions. *Clin. Oral Investig.* **2016**, *20*, 433–441.
15. Rajpal, S.; Sirohi, R. *Optical Methods of Measurement. Wholefield Techniques*, 2nd ed.; CRC Press, Taylor and Francis Group: Boca Raton, FL, USA, 2009.
16. Hecht, A.; Zajac, E. *Optics*; Addison Wesley Iberoamericana: Madrid, España, 2002.
17. Fuentes, M.V.; Ceballos, L.; González-López, S. Bond strength of self-adhesive resin cements to different treated indirect composites. *Clin. Oral Investig.* **2013**, *17*, 717–724. [CrossRef] [PubMed]
18. Inokoshi, M.; Nozaki, K.; Takagaki, T.; Okazaki, Y.; Yoshihara, K.; Minakuchi, S. Initial curing characteristics of composite cements under ceramic restorations. *J. Prosthodont. Res.* **2021**, *65*, 39–45. [CrossRef] [PubMed]
19. Ditchburn, R.W. *Light*, 3rd ed.; Academic Press: London, UK, 1976.

20. Sokal, R.; Rohlf, J. *Biometry*, 4th ed.; W.H. Freeman and Company: New York, NY, USA, 2011.
21. Valín, J.; Vinícius, P.; de Almeida, G.; Palacios, F.; Palacios, G.; Pérez, J.; Valín, M. Development of the Moiré method of projecting fringes for the evaluation of deformations in upper premolars. *Fund. Dialnet* **2017**, *20*, 22–30.